

Oxygen-isotope effect on density wave transitions in $\text{La}_3\text{Ni}_2\text{O}_7$

Rustem Khasanov,^{1,*} Vahid Sazgari,¹ Igor Plokhikh,^{1,2} Lifan Shi,³ KeYuan Ma,³ Marisa Medarde,¹ Ekaterina Pomjakushina,¹ Tomasz Klimczuk,^{4,5} Thomas J. Hicken,¹ Hubertus Luetkens,¹ Christof W. Schneieder,¹ Zurab Guguchia,¹ Sergey Medvedev,³ and Dariusz J. Gawryluk¹

¹PSI Center for Neutron and Muon Sciences CNM, 5232 Villigen PSI, Switzerland

²TU Dortmund University, Department of Physics, Dortmund, 44227, Germany

³Max Planck Institute for Chemical Physics of Solids, Nöthnitzer Strasse 40, 01187 Dresden, Germany

⁴Faculty of Applied Physics and Mathematics, Gdańsk University of Technology, Narutowicza 11/12, Gdansk, 80-233 Poland

⁵Advanced Materials Center, Gdańsk University of Technology, Narutowicza 11/12, Gdansk, 80-233 Poland

The isotope effect is a powerful probe of electron–phonon interactions in solid-state systems, offering key insights into how atomic mass influences emergent quantum states. Here, the impact of oxygen isotope substitution ($^{16}\text{O} \rightarrow ^{18}\text{O}$) on charge- and spin-density wave (CDW and SDW) transitions in the double-layer Ruddlesden–Popper nickelate $\text{La}_3\text{Ni}_2\text{O}_7$ is investigated. A clear isotope effect is observed in the CDW transition: the transition temperature (T_{CDW}) increases upon ^{18}O substitution. In contrast, the SDW transition temperature remains unaffected within experimental uncertainty. These findings point to a strong involvement of lattice vibrations in the formation of charge order, while spin order appears to be predominantly of electronic origin. The results suggest that electron–phonon coupling, manifested through the CDW response to isotope substitution, may be relevant to the superconducting pairing mechanism in Ruddlesden–Popper nickelates.

Introduction. The isotope effect was recognized as a fundamental tool in condensed matter physics for probing the intricate relationship between lattice vibrations and electronic properties. By replacing atoms with their isotopic counterparts, the role of phonons in various electronic and magnetic phase transitions can be assessed. This approach is particularly effective in differentiating phonon-driven phenomena from purely electronic interactions in complex materials.

Historically, the isotope effect was first observed in conventional superconductors, where it played a pivotal role in confirming the phonon-mediated pairing mechanism described by Bardeen–Cooper–Schrieffer (BCS) theory.^{1,2} In these materials, the superconducting transition temperature (T_c) follows the empirical relation $T_c \propto M^{-\alpha}$, where M represents the isotopic mass and the isotope exponent $\alpha \approx 0.5$ for an ideal phonon-mediated mechanism.^{3–17} This dependency arises because phonons mediate Cooper pair formation, and their characteristic frequencies scale as $M^{-1/2}$. However, significant deviations from this standard isotope effect was reported in strongly correlated electron systems, where additional interactions beyond conventional electron–phonon coupling are believed to contribute.^{13–15,17,18} In unconventional superconductors, the isotope effect varies significantly, suggesting a complex interplay between lattice vibrations and superconducting carriers.^{19–40}

Beyond superconductivity, isotope substitution was shown to influence the charge-density wave (CDW) and spin-density wave (SDW) transition temperatures in various materials.^{34,41–49} The formation of charge and spin-density waves arises due to collective electronic instabilities, often accompanied by lattice distortions, making these phases highly sensitive to phononic contributions. Variations in the density wave transition temperatures

(T_{CDW} and T_{SDW}) upon isotope substitution provide insight into the relative importance of electron–phonon interactions versus purely electronic effects in stabilizing these ordered states.

The recently discovered Ruddlesden–Popper (RP) nickelate superconductors exhibit a rich variety of electronic phases, with some of them potentially serving as precursors to superconductivity. In double- and tri-layer RP nickelates, charge density wave (CDW) and spin density wave (SDW) orders are observed at ambient pressure, while superconductivity emerges only under high-pressure conditions.^{50–67} Since superconductivity in these materials arises from states dominated by CDW and SDW correlations, investigating the isotope effect on both the precursor density wave orders and the superconducting phase offers valuable insights into the underlying pairing mechanism.

This work presents an investigation of the oxygen isotope effect (OIE) on the density-wave transition temperatures in the double-layer RP nickelate $\text{La}_3\text{Ni}_2\text{O}_7$. Our experiments reveal that the charge-density-wave transition is sensitive to isotope substitution, resulting in a higher transition temperature T_{CDW} for the sample containing the heavier oxygen isotope. The corresponding isotope shift, $\Delta T_{\text{CDW}} = T_{\text{CDW}}^{18} - T_{\text{CDW}}^{16}$, is approximately 2.3 K (throughout this study, superscripts ¹⁶ and ¹⁸ are used to indicate substitution with the corresponding oxygen isotope). In contrast, the isotope shift of the spin-density-wave transition temperature is negligible within experimental uncertainty, with $\Delta T_{\text{SDW}} = T_{\text{SDW}}^{18} - T_{\text{SDW}}^{16} = -0.08(9)$ K. These findings indicate that lattice vibrations play a significant role in the formation or stabilization of the CDW state, whereas the SDW transition appears to be governed predominantly by electronic interactions. The contrasting isotope responses of the CDW

and SDW transitions highlight the different microscopic origins of these ordered states in $\text{La}_3\text{Ni}_2\text{O}_7$ and provide useful constraints for theoretical models of density-wave formation in Ruddlesden–Popper nickelates.

Sample preparation and experimental techniques. The sample preparation procedure, as well as the experimental techniques used in the present study – namely x-ray diffraction, thermogravimetry, Raman spectroscopy, muon-spin rotation/relaxation (μSR), and resistivity – are described in the Supplemental Material part.⁶⁸

A schematic of the oxygen-isotope substitution apparatus is shown in Fig. S1(a) in the Supplemental Material, Ref. 68, and described in detail in Refs. 69,70. The ^{18}O content in the $\text{La}_3\text{Ni}_2^{18}\text{O}_{7\pm\delta}$ sample was determined to be 82(2)% using mass spectrometry analysis of the $^{18}\text{O}_2$ gas line.

X-ray diffraction experiments confirmed that the crystal structures of the ^{16}O - and ^{18}O -substituted sample pair remain unchanged. The results, including the symmetry group and lattice parameters (a , b , and c), are presented in Fig. S1(b) and Table S1 of the Supplemental Material.⁶⁸ Isotope substitution was found to have a negligible effect on all lattice parameters of $\text{La}_3\text{Ni}_2\text{O}_7$.

The oxygen content in the ^{16}O - and ^{18}O -substituted $\text{La}_3\text{Ni}_2\text{O}_{7\pm\delta}$ samples was determined using thermogravimetric analysis [Fig. S1(c) in the Supplemental Material, Ref. 68]. The samples were found to be nearly oxygen-stoichiometric, with oxygen contents ($7 \pm \delta$) determined to be 6.99(1) and 7.04(2) for $\text{La}_3\text{Ni}_2^{16}\text{O}_{7\pm\delta}$ and $\text{La}_3\text{Ni}_2^{18}\text{O}_{7\pm\delta}$, respectively. Hereafter, these samples are referred to as $\text{La}_3\text{Ni}_2^{16}\text{O}_7$ and $\text{La}_3\text{Ni}_2^{18}\text{O}_7$.

Oxygen-isotope effect on the phonon frequencies. Room-temperature Raman spectroscopy was employed to confirm both the effectiveness and spatial uniformity of ^{18}O isotope substitution, taking advantage of the technique’s sensitivity to mass-dependent shifts in phonon frequencies. The measured spectra, shown in Fig. 1 (a), were fitted using a sum of seven Lorentzian-shaped peaks. The extracted phonon frequencies for the ^{16}O - and ^{18}O -substituted $\text{La}_3\text{Ni}_2\text{O}_7$ samples, denoted as ν^{16} and ν^{18} , respectively, are listed in Table S2 in the Supplemental Material.⁶⁸

The coefficient representing the involvement of oxygen in each phonon mode, f_{O} , was calculated following Refs. 71–73:

$$\nu^{18}(x)/\nu^{16} = \left[\sqrt{M^{16}/M^{18}(x)} \right]^{f_{\text{O}}}, \quad (1)$$

where x is the ^{18}O content in the isotope-substituted sample (82% in this study), $M^{16} = 16$ is the atomic mass of ^{16}O , and $M^{18}(x) = (1-x) \cdot M^{16} + x \cdot M^{18}$ is the average oxygen mass in the ^{18}O -substituted sample. This relationship assumes a harmonic oscillator model, where mode softening upon isotope substitution reflects the oxygen contribution to each vibration.

Based on the extracted f_{O} values shown in Fig. 1 (b) and listed in Table S2 of the Supplemental Material,⁶⁸ the following conclusions can be drawn:

(i) Three phonon modes observed at ν^{16} (ν^{18}) = 368 (351), 549 (524), and 568 (542) cm^{-1} exhibit f_{O} values close to 1.0, indicating that these modes are dominated by oxygen vibrations.

(ii) The remaining modes at 161 (159), 226 (227), 269 (268), and 409 (398) cm^{-1} show significantly smaller – or even negligible, within experimental uncertainty – values of f_{O} , implying that oxygen is only weakly involved or not involved at all in these lattice vibrations. These modes are likely associated with heavier ions, such as Ni and La.

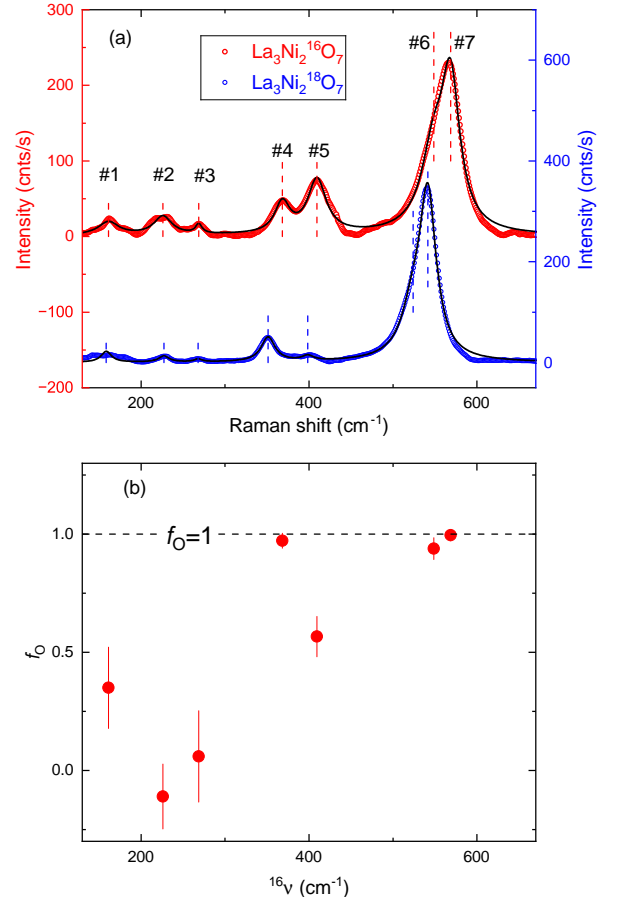


FIG. 1: (a) Room-temperature Raman spectra of oxygen-isotope substituted $\text{La}_3\text{Ni}_2\text{O}_7$ samples. Solid lines represent fits using seven Lorentzian functions. Dashed lines indicate the peak positions. (b) The oxygen participation parameter f_{O} as a function of the Raman wavenumber $^{16}\nu$.

Oxygen isotope effect on the CDW transition. The oxygen isotope effect on the CDW transition temperature was investigated via resistivity measurements. Figure 2 (a) shows the temperature dependence of resistivity normalized to its 300 K value, $R(T)/R(300)$. The raw resistivity curves exhibit weak anomalies near $T \sim 120$ K. A more pronounced structure emerges in the first derivative of the resistivity data, shown in Fig. 2 (b).

The anomalies observed in both the $R(T)/R(300)$ and $d[R(T)/R(300)]/dT$ curves may be attributed to charge- and spin-density wave transitions [dashed lines and gray

stripe in Figs. 2 (a) and (b)], as previously reported in the literature. The SDW transition at $T_{\text{SDW}} \simeq 150$ K was identified in earlier μSR , NMR, NQR, and resonant x-ray studies.^{67,74–81} Although the CDW in $\text{La}_3\text{Ni}_2\text{O}_7$ has not yet been directly confirmed by scattering techniques, anomalies in resistivity and specific heat at $110 \lesssim T \lesssim 130$ K have been associated with the onset of CDW order.^{53,60,82–85} Accordingly, an average CDW transition temperature of $T_{\text{CDW}} = 120$ K is adopted for $\text{La}_3\text{Ni}_2\text{O}_7$. It is also worth noting that recent optical pump-probe spectroscopy,⁸⁶ x-ray absorption near-edge spectroscopy,⁸⁷ and NQR⁸¹ measurements have provided further indications of CDW order below 150 K in $\text{La}_3\text{Ni}_2\text{O}_7$.

The isotope-induced shift of the CDW transition temperature was estimated using two approaches: (i) by determining the crossing point between linear fits to the derivative curves within the ‘slope’ and ‘plateau’ regions, which yielded $T_{\text{CDW}}^{16} = 117.7(2)$ K and $T_{\text{CDW}}^{18} = 120.2(2)$ K; and (ii) by identifying the crossing points of linear fits around the local minimum, giving $T_{\text{CDW}}^{16} = 103.6(1)$ K and $T_{\text{CDW}}^{18} = 105.8(1)$ K. Both approaches yield a consistent isotope shift of $\Delta T_{\text{CDW}} = T_{\text{CDW}}^{18} - T_{\text{CDW}}^{16} \simeq 2.4(2)$ K.

It should also be noted that the derivative curves exhibit a broad hump around 150 K, which may be associated with the SDW transition, as reported in Refs. 67,74–81. However, this feature is too broad to allow for a reliable determination of the OIE on T_{SDW} from resistivity data alone. Instead, the isotope effect on T_{SDW} is evaluated based on μSR measurements, presented below.

Oxygen isotope effect on the SDW transition. The OIE on the SDW transition temperature was investigated using μSR . Experiments were conducted in the weak-transverse field (WTF) mode with a magnetic field $B_{\text{WTF}} = 5$ mT applied perpendicular to the initial muon-spin polarization. The data analysis procedure, along with several WTF data sets, are provided in the Supplemental Material.⁶⁸

The temperature evolution of the magnetic volume fractions obtained from the fits to WTF- μSR data is presented in Fig. 3 (a). The dashed lines and grey stripe indicate the CDW and SDW transition temperatures, as reported in the literature.^{53,60,67,74,75,82–85,88,89} The WTF data clearly capture the SDW transition. It should be noted that the maximum value of the magnetic volume fraction does not reach 100%, which is attributed to approximately 5-7% of the muons missing the sample and stopping in the sample holder and/or the cryostat walls.

Figure 3 (b) shows an expanded view of the $f_m(T)$ curves in the vicinity of T_{SDW} . The SDW transition temperatures were estimated from the intersection of linearly extrapolated $f_m(T)$ curves near T_{SDW} with the reference line $f_m(T) = 0.5 \cdot f_m(10 \text{ K})$ [dashed lines in Fig. 3 (b)]. The fits yield $T_{\text{SDW}}^{16} = 150.44(6)$ K and $T_{\text{SDW}}^{18} = 150.36(6)$ K, resulting in an isotope shift of $\Delta T_{\text{SDW}} = T_{\text{SDW}}^{18} - T_{\text{SDW}}^{16} = -0.08(9)$ K.

Discussion and Conclusions. Table I summarizes the re-

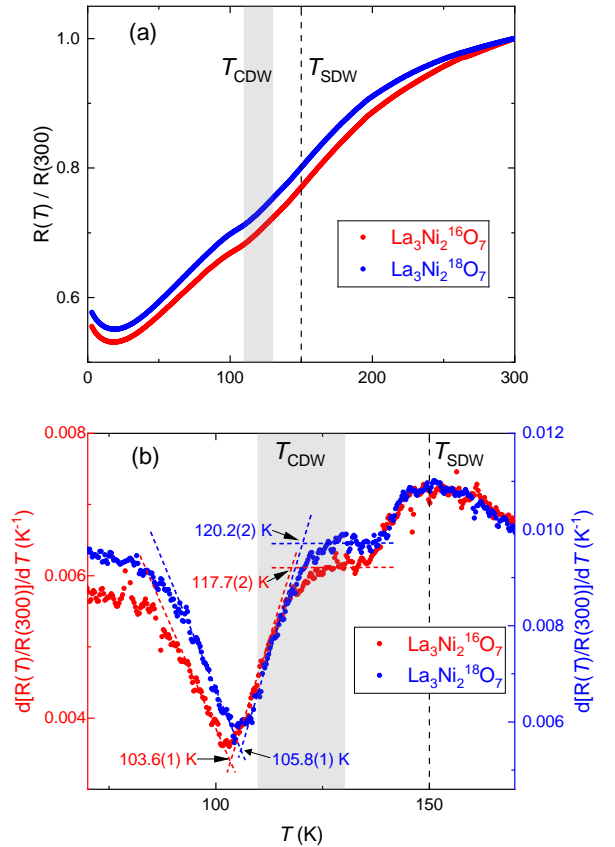


FIG. 2: (a) Raw resistivity curves of the $^{16}\text{O}/^{18}\text{O}$ -substituted $\text{La}_3\text{Ni}_2\text{O}_7$ samples. (b) Extended view of the first derivatives of the resistivity data in the vicinity of the CDW transitions. The red and blue numbers correspond to the CDW transition temperatures of $\text{La}_3\text{Ni}_2\text{ }^{16}\text{O}_7$ and $\text{La}_3\text{Ni}_2\text{ }^{18}\text{O}_7$, determined using different criteria (see text for details).

sults of the oxygen isotope effect measurements on the charge- and spin-density wave transition temperatures in the double-layer Ruddlesden–Popper nickelate $\text{La}_3\text{Ni}_2\text{O}_7$. The OIE results reported in the present study for $\text{La}_3\text{Ni}_2\text{O}_7$, together with those in Ref. 89 for the tri-layer RP nickelate $\text{La}_4\text{Ni}_3\text{O}_{10}$, can be directly compared to isotope effects investigated in cuprate high-temperature superconductors (HTSs), where such studies are among the most extensive within correlated electron systems.

In undoped cuprates, the isotope effect on the Néel temperature T_N is found to be negligible,^{34,44,46} consistent with the observations for $\text{La}_3\text{Ni}_2\text{O}_7$, where the SDW transition – preceding the CDW order – shows no measurable isotope shift. This suggests that magnetism, in the absence of strong charge fluctuations, is primarily governed by electronic interactions and is only weakly influenced by phonons.

In contrast, underdoped cuprates, where charge and spin orders coexist and are strongly correlated, show a different behavior. In stripe-ordered cuprates such as $\text{La}_{2-x}\text{Ba}_x\text{CuO}_4$, the emergence of static charge or-

TABLE I: Results of oxygen isotope effect measurements of $\text{La}_3\text{Ni}_2\text{O}_7$. $\Delta T_{tr} = T_{tr}^{18} - T_{tr}^{16}$ ($T_{tr} = T_{\text{SDW}}$ or T_{CDW}). The oxygen isotope exponent α is calculated by using equation $\alpha = -\ln T_{tr}/\ln M$ and is corrected for incomplete isotope exchange $\simeq 82\%$.

	$\text{La}_3\text{Ni}_2^{16}\text{O}_7$	$\text{La}_3\text{Ni}_2^{18}\text{O}_7$	ΔT_{tr}	α	Technique
T_{SDW}	150.44(6) K	150.36(6) K	-0.08(9) K	0.005(6)	WTF- μ SR
T_{CDW}	103.6(1) K ^a	105.8(1) K ^a	2.2(1) K	-0.21(1)	Resistivity
	117.7(2) K ^b	120.2(2) K ^b	2.5(4) K	-0.21(3)	Resistivity

^aFrom local minima at $d[R(T)/R(300)]/dT$ [Fig. 2 (b)]

^bFrom linear slopes of $d[R(T)/R(300)]/dT$ [Fig. 2 (b)]

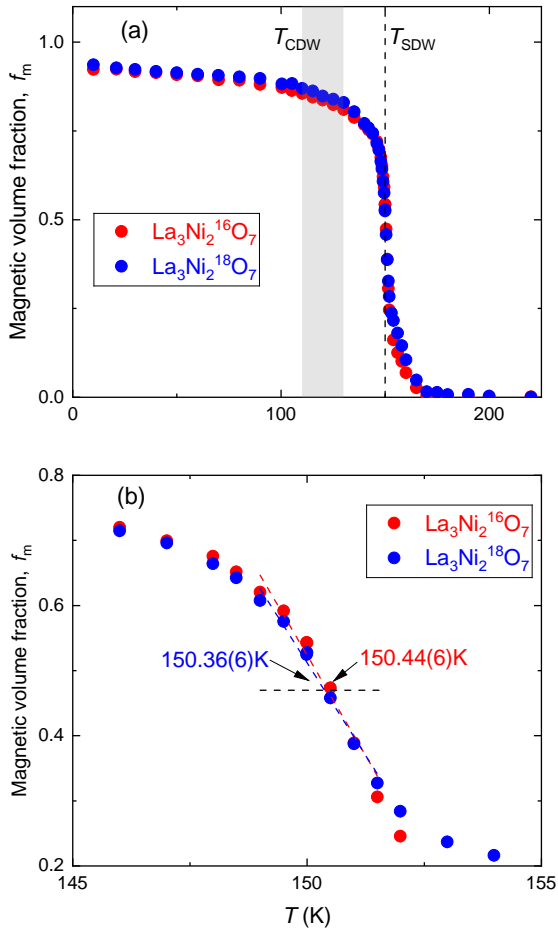


FIG. 3: (a) Temperature dependence of the magnetic volume fraction f_m for ^{16}O - and ^{18}O -substituted $\text{La}_3\text{Ni}_2\text{O}_7$ and $\text{La}_4\text{Ni}_3\text{O}_{10}$ samples. (b) Extended view of the $f_m(T)$ curves in the vicinity of the SDW transitions. The vertical dashed lines and grey stripe indicate the CDW and SDW transition temperatures (T_{CDW} and T_{SDW}), as reported in the literature.^{53,60,67,74,75,82–85,88,89}

der is accompanied by a spin-stripe phase that strongly suppresses superconductivity.^{90–97} Notably, isotope effect studies in these systems show that both the CDW and SDW transition temperatures increase upon ^{18}O substitution, with shifts of the same sign and comparable magnitude.^{41,48}

This behavior is strikingly similar to the findings in

$\text{La}_4\text{Ni}_3\text{O}_{10}$,⁸⁹ where CDW and SDW orders are intertwined, share the same transition temperature ($T_{\text{CDW}} \simeq T_{\text{SDW}}$), and exhibit identical isotope shifts ($\Delta T_{\text{CDW}} = \Delta T_{\text{SDW}}$). These parallels suggest a shared underlying mechanism, likely involving strong electron–phonon coupling that affects both spin and charge degrees of freedom when the two orders are strongly entangled.

Despite these parallels, there are notable differences between cuprates and nickelates. In cuprate HTSs, increasing hole doping suppresses the SDW order, eventually leading to the emergence of superconductivity,^{98–100} while in $\text{La}_3\text{Ni}_2\text{O}_7$, applying pressure does not immediately suppress SDW order.⁶⁷ Moreover, in $\text{La}_4\text{Ni}_3\text{O}_{10}$, the SDW order does not appear to be the primary instability, but rather a consequence of CDW formation.⁸⁹

In kagome materials, such as CsV_3Sb_5 , KV_3Sb_5 , and RbV_3Sb_5 , suppression of CDW order through pressure or chemical tuning was found to enhance superconductivity.^{101–105} A similar trend may be expected in nickelates, where superconductivity emerges under high pressure and is associated with the suppression of charge order. This raises the possibility that, as in kagome superconductors, CDW order plays the dominant role in competing with superconductivity in RP nickelates, rather than SDW order.

To conclude, our findings reveal that the CDW and SDW transitions in $\text{La}_3\text{Ni}_2\text{O}_7$ exhibit markedly different sensitivities to oxygen-isotope substitution. The clear isotope dependence of the CDW transition highlights a strong coupling between charge order and lattice vibrations, while the SDW transition shows no measurable isotope shift, indicating a predominantly electronic origin. This distinct isotope response offers valuable insight into the role of electron–phonon interactions and electronic correlations in layered nickelates, and demonstrates that isotope substitution is an effective tool for disentangling competing ordered states in Ruddlesden–Popper systems.

Acknowledgments Z.G. acknowledges support from the Swiss National Science Foundation (SNSF) through SNSF Starting Grant (No. TMSGI2.211750). I.P. acknowledges financial support from Paul Scherrer Institute research grant No. 2021_0134. D.J.G. acknowledges support from the Swiss National Science Foundation (SNSF) through Grant No. 200021E_238113.

- * Electronic address: rustem.khasanov@psi.ch
- ¹ H. Fröhlich, *Theory of the Superconducting State. I. The Ground State at the Absolute Zero of Temperature*, Phys. Rev. **79**, 845 (1950).
<https://doi.org/10.1103/PhysRev.79.845>
 - ² J. Bardeen, L. N. Cooper, and J. R. Schrieffer, *Theory of Superconductivity*, Phys. Rev. **108**, 1175 (1957).
<https://doi.org/10.1103/PhysRev.108.1175>
 - ³ Emanuel Maxwell, *Isotope Effect in the Superconductivity of Mercury*, Phys. Rev. **78**, 477 (1950).
<https://doi.org/10.1103/PhysRev.78.477>
 - ⁴ C. A. Reynolds, B. Serin, and L. B. Nesbitt, *The Isotope Effect in Superconductivity. I. Mercury*, Phys. Rev. **84**, 691 (1951).
<https://doi.org/10.1103/PhysRev.84.691>
 - ⁵ J.L. Olsen, Superconductivity of cadmium isotopes, *Cryogenics* **2**, 356 (1963).
[https://doi.org/10.1016/0011-2275\(62\)90078-4](https://doi.org/10.1016/0011-2275(62)90078-4)
 - ⁶ R. W. Shaw, D. E. Mapother, and D. C. Hopkins, *Isotope Effect in Superconducting Lead*, Phys. Rev. **121**, 86 (1961).
<https://doi.org/10.1103/PhysRev.121.86>
 - ⁷ B. T. Mathias, T. H. Geballe, E. Corenzwit and G. W. Hull Jr., *Intermediate Isotope Effect of Molybdenum and Mo_3Ir* Phys. Rev. **129**, 1025 (1963).
<https://doi.org/10.1103/PhysRev.129.1025>
 - ⁸ E. Bucher and C. Palmy, *Superconductivity and isotope effect in Be_{22}X compounds and molybdenum*, Phys. Letters A **24**, 340 (1967).
[https://doi.org/10.1016/0375-9601\(67\)90913-9](https://doi.org/10.1016/0375-9601(67)90913-9)
 - ⁹ R. E. Fasnacht and J. R. Dillinge, *Isotope Effect in Superconducting Zinc*, Phys. Rev. Letters **17**, 255 (1966).
<https://doi.org/10.1103/PhysRevLett.17.255>
 - ¹⁰ S. L. Bud'ko, G. Lapertot, C. Petrovic, C. E. Cunningham, N. Anderson, and P. C. Canfield, *Boron Isotope Effect in Superconducting MgB_2* , Phys. Rev. Lett. **86**, 1877 (2001).
<https://doi.org/10.1103/PhysRevLett.86.1877>
 - ¹¹ D. G. Hinks, H. Clauss and J. D. Jorgensen, *The complex nature of superconductivity in MgB_2 as revealed by the reduced total isotope effect*, Nature **411**, 457 (2001).
<https://doi.org/10.1038/35078037>
 - ¹² R. A. Hein and J. W. Gibson, *Isotope Effect in Superconducting Osmium*, Phys. Rev. **131**, 1105 (1963).
<https://doi.org/10.1103/PhysRev.131.1105>
 - ¹³ T. H. Geballe, B. T. Mathias, G. W. Hull Jr. and E. Corenzwit, *Absence of an Isotope Effect in Superconducting Ruthenium*, Phys. Rev. Letters **6**, 275 (1961).
<https://doi.org/10.1103/PhysRevLett.6.275>
 - ¹⁴ D. K. Finnemore and D. E. Mapother, *Absence of an Isotope Effect in Superconducting Ruthenium*, Phys. Rev. Letters **9**, 288 (1962).
<https://doi.org/10.1103/PhysRevLett.9.288>
 - ¹⁵ J. W. Gibson and R. A. Hein, *Critical Magnetic Fields of Superconducting Ruthenium Isotopes and Search for an Isotope Effect*, Phys. Rev. **141**, 407 (1966).
<https://doi.org/10.1103/PhysRev.141.407>
 - ¹⁶ T. H. Geballe and B. T. Mathias, *Isotope Effects in Low Temperature Superconductors*, IBM J. Res. Develop **6**, 256 (1962).
<https://doi.org/10.1147/rd.62.0256>
 - ¹⁷ R. D. Fowler, J. D. G. Linsday, R. W. White, H. H. Hill and B.T.Mathias, *Positive Isotope Effect on the Superconducting Transition Temperature of α -Uranium*, Phys. Rev. Letters **19**, 892 (1967).
<https://doi.org/10.1103/PhysRevLett.19.892>
 - ¹⁸ B. Stritzker and W. Buckel, *Superconductivity in the palladium-hydrogen and the palladium-deuterium systems*, Z. Physik **257**, 1 (1972).
<https://doi.org/10.1007/BF01398191>
 - ¹⁹ B. Batlogg, G. Kourouklis, W. Weber, R. J. Cava, A. Jayaraman, A. E. White, K. T. Short, L. W. Rupp, and E. A. Rietman, *Nonzero isotope effect in $\text{La}_{1.85}\text{Sr}_{0.15}\text{CuO}_4$* , Phys. Rev. Lett. **59**, 912 (1987).
<https://doi.org/10.1103/PhysRevLett.59.912>
 - ²⁰ Tanya A. Faltens, William K. Ham, Steven W. Keller, Kevin J. Leary, James N. Michaels, Angelica M. Stacy, Hans-Conrad zur Loye, Donald E. Morris, T. W. Barbee III, L. C. Bourne, Marvin L. Cohen, S. Hoen, and A. Zettl, *Observation of an oxygen isotope shift in the superconducting transition temperature of $\text{La}_{1.85}\text{Sr}_{0.15}\text{CuO}_4$* , Phys. Rev. Lett. **59**, 915 (1987).
<https://doi.org/10.1103/PhysRevLett.59.915>
 - ²¹ B. Batlogg, R. J. Cava, A. Jayaraman, R. B. van Dover, G. A. Kourouklis, S. Sunshine, D. W. Murphy, L. W. Rupp, H. S. Chen, A. White, K. T. Short, A. M. Mujsce, and E. A. Rietman, *Isotope Effect in the High- T_c Superconductors $\text{Ba}_2\text{YCu}_3\text{O}_7$ and $\text{Ba}_2\text{EuCu}_3\text{O}_7$* , Phys. Rev. Lett. **58**, 2333 (1987).
<https://doi.org/10.1103/PhysRevLett.58.2333>
 - ²² L. C. Bourne, M. F. Crommie, A. Zettl, Hans-Conrad zur Loye, S. W. Keller, K. L. Leary, Angelica M. Stacy, K. J. Chang, Marvin L. Cohen, and Donald E. Morris, *Search for Isotope Effect in Superconducting Y-Ba-Cu-O*, Phys. Rev. Lett. **58**, 2337 Phys. Rev. Lett. **59**, 1492 (1987).
<https://doi.org/10.1103/PhysRevLett.58.2337>
 - ²³ J. P. Franck, J. Jung, M. A.-K. Mohamed, S. Gygax, and G. I. Sproule, *Observation of an oxygen isotope effect in superconducting $(\text{Y}_{1-x}\text{Pr}_x)\text{Ba}_3\text{Cu}_3\text{O}_{7-\delta}$* , Phys. Rev. B **44**, 5318 (1991).
<https://doi.org/10.1103/PhysRevB.44.5318>
 - ²⁴ N. Babushkina, A. Inyushkin, V. Ozhogin, A. Taldenkov, I. Kobrin, T. Vorobeva, L. Molchanova, L. Damyanets, T. Uvarova, and A. Kuzakov, *Oxygen isotope effect in LaSrCuO system with T_c modified by Ni and Zn doping*, Physica C **185-189**, 901 (1991).
[https://doi.org/10.1016/0921-4534\(91\)91674-S](https://doi.org/10.1016/0921-4534(91)91674-S)
 - ²⁵ Guo-meng Zhao, M. B. Hunt, H. Keller, and K. A. Müller, *Evidence for polaronic supercarriers in the copper oxide superconductors $\text{La}_{2-x}\text{Sr}_x\text{CuO}_4$* , Nature volume **385**, 236 (1997).
<https://doi.org/10.1038/385236a0>
 - ²⁶ D. Zech, H. Keller, K. Conder, E. Kaldis, E. Liarakapis, N. Poulakis, and K. A. Müller, *Site-selective oxygen isotope effect in optimally doped $\text{YBa}_2\text{Cu}_3\text{O}_{6+x}$* , Nature **371**, 681 (1994).
<https://doi.org/10.1038/371681a0>
 - ²⁷ D. Zech, K. Conder, H. Keller, E. Kaldis, and K.A. Müller, *Doping dependence of the oxygen isotope effect in $\text{YBa}_2\text{Cu}_3\text{O}_x$* , Physica B **219**, 136 (1996).
[https://doi.org/10.1016/0921-4526\(95\)00674-5](https://doi.org/10.1016/0921-4526(95)00674-5)
 - ²⁸ R. Khasanov, A. Shengelaya, E. Morenzoni, M. Angst,

- K. Conder, I. M. Savić, D. Lampakis, E. Liarokapis, A. Tatsi, and H. Keller, *Site-selective oxygen isotope effect on the magnetic-field penetration depth in underdoped $Y_{0.6}Pr_{0.4}Ba_2Cu_3O_{7-\delta}$* , Phys. Rev. B **68**, 220506(R) (2003).
<https://doi.org/10.1103/PhysRevB.68.220506>
- ²⁹ J. L. Tallon, R. S. Islam, J. Storey, G. V. M. Williams¹, and J. R. Cooper, *Isotope Effect in the Superfluid Density of High-Temperature Superconducting Cuprates: Stripes, Pseudogap, and Impurities*, Phys. Rev. Lett. **94**, 237002 (2005).
<https://doi.org/10.1103/PhysRevLett.94.237002>
- ³⁰ H. Keller, A. Bussmann-Holder, K. A. Müller, Mater. Today **11**, 38 (2008).
[https://doi.org/10.1016/s1369-7021\(08\)70178-0](https://doi.org/10.1016/s1369-7021(08)70178-0)
- ³¹ R. Khasanov, D. G. Eshchenko, H. Luetkens, E. Morenzoni, T. Prokscha, A. Suter, N. Garifianov, M. Mali, J. Roos, K. Conder, and H. Keller, *Direct Observation of the Oxygen Isotope Effect on the In-Plane Magnetic Field Penetration Depth in Optimally Doped $YBa_2Cu_3O_{7-\delta}$* , Phys. Rev. Lett. **92**, 057602 (2004).
<https://doi.org/10.1103/PhysRevLett.92.057602>
- ³² Z. Q. Mao, Y. Maeno, Y. Mori, S. Sakita, S. Nimori, and M. Udagawa, *Sign reversal of the oxygen isotope effect on T_c in Sr_2RuO_4* , Phys. Rev. B **63**, 144514 (2001).
<https://doi.org/10.1103/PhysRevB.63.144514>
- ³³ R. Khasanov, A. Shengelaya, K. Conder, E. Morenzoni, I. M. Savić, J. Karpinski, and H. Keller, *Correlation between oxygen isotope effects on transition temperature and magnetic penetration depth in high-temperature superconductors close to optimal doping*, Phys. Rev. B **74**, 064504 (2006).
<https://doi.org/10.1103/PhysRevB.74.064504>
- ³⁴ R. Khasanov, A. Shengelaya, D. Di Castro, E. Morenzoni, A. Maisuradze, I. M. Savić, K. Conder, E. Pomjakushina, A. Bussmann-Holder, and H. Keller, *Oxygen isotope effects on the superconducting transition and magnetic states within the phase Ddagram of $Y_{1-x}Pr_xBa_2Cu_3O_{7-\delta}$* , Phys. Rev. Lett. **101**, 077001 (2008).
<https://doi.org/10.1103/PhysRevLett.101.077001>
- ³⁵ C. W. Rischau, D. Pulmannová, G. W. Scheerer, A. Stucky, E. Giannini, and D. van der Marel, *Isotope tuning of the superconducting dome of strontium titanate*, Phys. Rev. Research **4**, 013019 (2022).
<https://doi.org/10.1103/PhysRevResearch.4.013019>
- ³⁶ J. A. Schlueter, A. M. Kini, B. H. Ward, U. Geiser, H. H. Wang, J. Mohtasham, R. W. Winter, G. L. Gard, *Universal inverse deuterium isotope effect on the T_c of BEDT-TTF-based molecular superconductors*, Physica C **351**, 261 (2001).
[https://doi.org/10.1016/S0921-4534\(00\)01620-8](https://doi.org/10.1016/S0921-4534(00)01620-8)
- ³⁷ R. H. Liu, T. Wu, G. Wu, H. Chen, X. F. Wang, Y. L. Xie, J. J. Yin, Y. J. Yan, Q. J. Li, B. C. Shi, W. S. Chu, Z. Y. Wu, and X. H. Chen, *A large iron isotope effect in $SmFeAsO_{1-x}F_x$ and $Ba_{1-x}K_xFe_2As_2$* , Nature **459** 64, (2009).
<https://doi.org/10.1038/nature07981>
- ³⁸ P. M. Shirage, K. Kihou, K. Miyazawa, C.-H. Lee, H. Kito, H. Eisaki, Y. Tanaka, and A. Iyo, *Inverse Iron Isotope Effect on the Transition Temperature of the $(BaK)_2Fe_2As_2$ Superconductor*, Phys. Rev. Lett. **103**, 257003 (2009).
<https://doi.org/10.1103/PhysRevLett.103.257003>
- ³⁹ R. Khasanov, M. Bendele, K. Conder, H. Keller, E. Pomjakushina and V. Pomjakushin, *Iron isotope effect on the superconducting transition temperature and the crystal structure of $FeSe_{1-x}$* , New J. Phys. **12** 073024 (2010).
<https://doi.org/10.1088/1367-2630/12/7/073024>
- ⁴⁰ R. Khasanov, M. Bendele, A. Bussmann-Holder, and H. Keller, *Intrinsic and structural isotope effects in iron-based superconductors*, Phys. Rev. B **82**, 212505 (2010).
<https://doi.org/10.1103/PhysRevB.82.212505>
- ⁴¹ Z. Guguchia, R. Khasanov, M. Bendele, E. Pomjakushina, K. Conder, A. Shengelaya, and H. Keller, *Negative Oxygen Isotope Effect on the Static Spin Stripe Order in Superconducting $La_{2-x}Ba_xCuO_4$ ($x = 1/8$) Observed by Muon Spin Rotation*, Phys. Rev. Lett. **113**, 057002 (2014).
<https://doi.org/10.1103/PhysRevLett.113.057002>
- ⁴² M. Medarde, P. Lacorre, K. Conder, F. Fauth, and A. Furrer, *Giant $^{16}O-^{18}O$ Isotope Effect on the Metal-Insulator Transition of $RNiO_3$ Perovskites ($R = \text{Rare Earth}$)*, Phys. Rev. Lett. **80**, 2397 (1998).
<https://doi.org/10.1103/PhysRevLett.80.2397>
- ⁴³ H. Luetkens, M. Stingaciu, Y.G. Pashkevich, P. Lemmens, E. Pomjakushina, K. Conder, and H.-H. Klauss, *Oxygen isotope effect on the AFM-FM phase transition of the layered cobaltite $HoBaCo_2O_{5.47}$* , J. Magn. Magn. Mater. **310**, 1566 (2007).
<https://doi.org/10.1016/j.jmmm.2006.10.596>
- ⁴⁴ E. Amit, A. Keren, J.S. Lord, and P. A. King, *Precise Measurement of the Oxygen Isotope Effect on the Néel Temperature in Cuprates*, Advances in Condensed Matter Physics **1**, 178190 (2011).
<https://doi.org/10.1155/2011/178190>
- ⁴⁵ A. Shengelaya, Guo-meng Zhao, C. M. Aegerter, K. Conder, I. M. Savić, and H. Keller, *Giant Oxygen Isotope Effect on the Spin Glass Transition in $La_{2-x}Sr_xCu_{1-z}Mn_zO_4$ as Revealed by Muon Spin Rotation*, Phys. Rev. Lett. **83**, 5142 (1999).
<https://doi.org/10.1103/PhysRevLett.83.5142>
- ⁴⁶ Guo-meng Zhao, K. K. Singh, and Donald E. Morris, *Oxygen isotope effect on Néel temperature in various antiferromagnetic cuprates*, Phys. Rev. B **50**, 4112 (1994).
<https://doi.org/10.1103/PhysRevB.50.4112>
- ⁴⁷ A. Lanzara, Guo-meng Zhao, N. L. Saini, A. Bianconi, K. Conder, H. Keller and K. A. Müller, *Oxygen-isotope shift of the charge-stripe ordering temperature in $la_{2-x}Sr_xCuO_4$ from x-ray absorption spectroscopy*, J. Phys.: Condens. Matter **11** L541 (1999).
<https://doi.org/10.1088/0953-8984/11/48/103>
- ⁴⁸ Z. Guguchia, D. Sheptyakov, E. Pomjakushina, K. Conder, R. Khasanov, A. Shengelaya, A. Simon, A. Bussmann-Holder, and H. Keller, *Oxygen isotope effects on lattice properties of $La_{2-x}Ba_xCuO_4$ ($x = 1/8$)*, Phys. Rev. B **92**, 024508 (2015).
<https://doi.org/10.1103/PhysRevB.92.024508>
- ⁴⁹ M. Bendele, F. von Rohr, Z. Guguchia, E. Pomjakushina, K. Conder, A. Bianconi, A. Simon, A. Bussmann-Holder, and H. Keller, *Evidence for strong lattice effects as revealed from huge unconventional oxygen isotope effects on the pseudogap temperature in $La_{2-x}Sr_xCuO_4$* , Phys. Rev. B **95**, 014514 (2017).
<https://doi.org/10.1103/PhysRevB.95.014514>
- ⁵⁰ Hualei Sun, Mengwu Huo, Xunwu Hu, Jingyuan Li, Zengjia Liu, Yifeng Han, Lingyun Tang, Zhongquan Mao, Pengtao Yang, Bosen Wang, Jinguang Cheng, Dao-Xin Yao, Guang-Ming Zhang, and Meng Wang, *Signatures of superconductivity near 80 K in a nickelate under high*

- pressure, *Nature* **621**, 493 (2023).
<https://doi.org/10.1038/s41586-023-06408-7>
- ⁵¹ Yanan Zhang, Dajun Su, Yanen Huang, Zhaoyang Shan, Hualei Sun, Mengwu Huo, Kaixin Ye, Jiawen Zhang, Zihan Yang, Yongkang Xu, Yi Su, Rui Li, Michael Smidman, Meng Wang, Lin Jiao, and Huiqiu Yuan, *High-temperature superconductivity with zero resistance and strange-metal behaviour in $La_3Ni_2O_{7-\delta}$* , *Nat. Phys.* **20**, 1269, (2024).
<https://doi.org/10.1038/s41586-024-02515-y>
- ⁵² Ningning Wang, Gang Wang, Xiaoling Shen, Jun Hou, Jun Luo, Xiaoping Ma, Huaixin Yang, Lifan Shi, Jie Dou, Jie Feng, Jie Yang, Yunqing Shi, Zhian Ren, Hanming Ma, Pengtao Yang, Ziyi Liu, Yue Liu, Hua Zhang, Xiaoli Dong, Yuxin Wang, Kun Jiang, Jiangping Hu, Shoko Nagasaki, Kentaro Kitagawa, Stuart Calder, Jiaqiang Yan, Jianping Sun, Bosen Wang, Rui Zhou, Yoshiya Uwatoko, and Jinguang Cheng, *Bulk high-temperature superconductivity in pressurized tetragonal $La_2PrNi_2O_7$* , *Nature* **634**, 579 (2024).
<https://doi.org/10.1038/s41586-024-07996-8>
- ⁵³ Zhe Liu, Mengwu Huo, Jie Li, Qing Li, Yuecong Liu, Yaomin Dai, Xiaoxiang Zhou, Jiahao Hao, Yi Lu, Meng Wang, and Hai-Hu Wen, *Electronic correlations and energy gap in the bilayer nickelate $La_3Ni_2O_7$* , *Nat. Commun.* **15**, 7570 (2024).
<https://doi.org/10.1038/s41467-024-52001-5>
- ⁵⁴ Mingxin Zhang, Cuiying Pei, Qi Wang, Yi Zhao, Changhua Li, Weizheng Cao, Shihao Zhu, Juefei Wu, and Yanpeng Qi, *Effects of pressure and doping on Ruddlesden-Popper phases $La_{n+1}Ni_nO_{3n+1}$* , *J. Mater. Sci. Technol.* **185**, 147, (2024).
<https://doi.org/10.1016/j.jmst.2023.11.011>
- ⁵⁵ Yidian Li, Yantao Cao, Liangyang Liu, Pai Peng, Hao Lin, Cuiying Pei, Mingxin Zhang, Heng Wu, Xian Du, Wenxuan Zhao, Kaiyi Zhai, Zhang Xuefeng, Jinkui Zhao, Miaoling Lin, Pingheng Tan, Yanpeng Qi, Gang Li, Guo Hanjie, Luyi Yang, Lexian Yang, *Distinct ultrafast dynamics of bilayer and trilayer nickelate superconductors regarding the density-wave-like transitions*, *Sci. Bull.* **70**, 180 (2024).
<https://doi.org/10.1016/j.scib.2024.10.011>
- ⁵⁶ Yidian Li, Xian Du, Yantao Cao, Cuiying Pei, Mingxin Zhang, Wenxuan Zhao, Kaiyi Zhai, Runzhe Xu, Zhongkai Liu, Zhiwei Li, Jinkui Zhao, Gang Li, Yanpeng Qi, Hanjie Guo, Yulin Chen, and Lexian Yang, *Electronic Correlation and Pseudogap-Like Behavior of High-Temperature Superconductor $La_3Ni_2O_7$* , *Chinese Phys. Lett.* **41**, 087402, (2024).
<https://doi.org/10.1088/0256-307X/41/8/087402>
- ⁵⁷ Yazhou Zhou, Jing Guo, Shu Cai, Hualei Sun, Pengyu Wang, Jinyu Zhao, Jinyu Han, Xintian Chen, Yongjin Chen, Qi Wu, Yang Ding, Tao Xiang, Ho-kwang Mao, Liling Sun *Investigations of key issues on the reproducibility of high T_c superconductivity emerging from compressed $La_3Ni_2O_7$* , *Matter Radiat. Extremes* **10**, 027801(2025).
<https://doi.org/10.1063/5.0247684>
- ⁵⁸ Xiaoxiang Zhou, Weihong He, Zijian Zhou, Kaipeng Ni, Mengwu Huo, Deyuan Hu, Yinghao Zhu, Enkang Zhang, Zhicheng Jiang, Shuaikang Zhang, Shiwu Su, Juan Jiang, Yajun Yan, Yilin Wang, Dawei Shen, Xue Liu, Jun Zhao, Meng Wang, Mengkun Liu, Zengyi Du, and Donglai Feng, *Revealing nanoscale structural phase separation in $La_3Ni_2O_{7-\delta}$ single crystal via scanning near field optical microscopy*, arXiv:2410.06602 (2024).
<https://doi.org/10.48550/arXiv.2410.06602>
- ⁵⁹ Hirofumi Sakakibara, Masayuki Ochi, Hibiki Nagata, Yuta Ueki, Hiroya Sakurai, Ryo Matsumoto, Kensei Terashima, Keisuke Hirose, Hiroto Ohta, Masaki Kato, Yoshihiko Takano, and Kazuhiko Kuroki, *Theoretical analysis on the possibility of superconductivity in the trilayer Ruddlesden-Popper nickelate $La_4Ni_3O_{10}$ under pressure and its experimental examination: Comparison with $La_3Ni_2O_7$* , *Phys. Rev. B* **109**, 144511, (2024).
<https://doi.org/10.1103/PhysRevB.109.144511>
- ⁶⁰ Meng Wang, Hai-Hu Wen, Tao Wu, Dao-Xin Yao, and Tao Xiang, *Normal and superconducting properties of $La_3Ni_2O_7$* , *Chinese Phys. Lett.* **41**, 077402, (2024).
<https://doi.org/10.1088/0256-307X/41/7/077402>
- ⁶¹ Cuiying Pei, Mingxin Zhang, Di Peng, Shangxiong Huangfu, Shihao Zhu, Qi Wang, Juefei Wu, Zhenfang Xing, Lili Zhang, Yulin Chen, Jinkui Zhao, Wenge Yang, Hongli Suo, Hanjie Guo, Qiaoshi Zeng, Yanpeng Qi, *Pressure-Induced Superconductivity in $Pr_4Ni_3O_{10}$ Single Crystals*, arXiv:2411.08677v1.
<https://doi.org/10.48550/arXiv.2411.08677>
- ⁶² G. Wang, N. N. Wang, X. L. Shen, J. Hou, L. Ma, L. F. Shi, Z. A. Ren, Y. D. Gu, H. M. Ma, P. T. Yang, Z. Y. Liu, H. Z. Guo, J. P. Sun, G. M. Zhang, S. Calder, J.-Q. Yan, B. S. Wang, Y. Uwatoko, and J.-G. Cheng, *Pressure-Induced Superconductivity In Polycrystalline $La_3Ni_2O_{7-\delta}$* , *Phys. Rev. X* **14**, 011040 (2024).
<https://doi.org/10.1103/PhysRevX.14.011040>
- ⁶³ Feiyu Li, Yinqiao Hao, Ning Guo, Jian Zhang, Qiang Zheng, Guangtao Liu, and Junjie Zhang, *Signature of superconductivity in pressurized $La_4Ni_3O_{10-x}$ single crystals grown at ambient pressure*, arXiv:2501.13511v1 (2025).
<https://doi.org/10.48550/arXiv.2501.13511>
- ⁶⁴ P. Puphal, P. Reiss, N. Enderlein, Y.-M. Wu, G. Khalullin, V. Sundaramurthy, T. Priessnitz, M. Knauff, A. Suthar, L. Richter, M. Isobe, P. A. van Aken, H. Takagi, B. Keimer, Y. E. Suyolcu, B. Wehinger, P. Hansmann, and M. Hepting, *Unconventional Crystal Structure of the High-Pressure Superconductor $La_3Ni_2O_7$* , *Phys. Rev. Lett.* **133**, 146002 (2024).
<https://doi.org/10.1103/PhysRevLett.133.146002>
- ⁶⁵ Yinghao Zhu, Di Peng, Enkang Zhang, Bingying Pan, Xu Chen, Lixing Chen, Huifen Ren, Feiyang Liu, Yiqing Hao, Nana Li, Zhenfang Xing, Fujun Lan, Jiyan Han, Junjie Wang, Donghan Jia, Hongliang Wo, Yiqing Gu, Yimeng Gu, Li Ji, Wenbin Wang, Huiyang Gou, Yao Shen, Tianping Ying, Xiaolong Chen, Wenge Yang, Huibo Cao, Changlin Zheng, Qiaoshi Zeng, Jian-gang Guo, and Jun Zhao, *Superconductivity in pressurized trilayer $La_4Ni_3O_{10-\delta}$ single crystals*, *Nature* **631**, 531 (2024).
<https://doi.org/10.1038/s41586-024-07553-3>
- ⁶⁶ Enkang Zhang, Di Peng, Yinghao Zhu, Lixing Chen, Bingkun Cui, Xingya Wang, Wenbin Wang, Qiaoshi Zeng, and Jun Zhao, *Bulk Superconductivity in Pressurized Trilayer Nickelate $Pr_4Ni_3O_{10}$ Single Crystals*, *Phys. Rev. X* **15**, 021008 (2025).
<https://doi.org/10.1103/PhysRevX.15.021008>
- ⁶⁷ Rustem Khasanov, Thomas J. Hicken, Dariusz J. Gawryluk, Vahid Sazgari, Igor Plokhikh, Loïc Pierre Sorel, Marek Bartkowiak, Steffen Bötzel, Frank Lechermann, Ilya M. Eremin, Hubertus Luetkens, Zurab Guguchia, *Pressure-enhanced splitting of density wave transitions in $La_3Ni_2O_{7-\delta}$* , *Nat. Phys.* (2025).

- <https://doi.org/10.1038/s41567-024-02754-z>
- ⁶⁸ The Supplemental Material contains details of the sample preparation procedures, as well as descriptions of the experimental techniques used in this study, namely x-ray diffraction, thermogravimetry, Raman spectroscopy, muon-spin rotation/relaxation (μ SR), and resistivity measurements. In addition to the references cited in the main text, it includes Refs. 106–114.
- ⁶⁹ Kazimierz Conder, *Oxygen diffusion in the superconductors of the YBaCuO family: isotope exchange measurements and models*, Mater. Sci. Eng. **R32**, 41 (2001). [https://doi.org/10.1016/S0927-796X\(00\)00030-9](https://doi.org/10.1016/S0927-796X(00)00030-9)
- ⁷⁰ K. Conder, *Material aspects of oxygen isotope effect studies in high-temperature superconductors*, Physica C **614**, 1354316 (2023). <https://doi.org/10.1016/j.physc.2023.1354376>
- ⁷¹ Manuel Cardona and M. L. W. Thewalt, *Isotope effects on the optical spectra of semiconductors*, Rev. Mod. Phys. **77**, 1173 (2005). DOI:<https://doi.org/10.1103/RevModPhys.77.1173>
- ⁷² J. Menéndez, J. B. Page, and S. Guha, *The isotope effect on the Raman spectrum of molecular C₆₀*, Philosophical Magazine B, **70**, 651 (1994). <https://doi.org/10.1080/01418639408240239>
- ⁷³ J. M. Zhang, T. Ruf, M. Cardona, O. Ambacher, M. Stutzmann, J.-M. Wagner, and F. Bechstedt, *Raman spectra of isotopic GaN*, Phys. Rev. B **56**, 14399 (1997). DOI:<https://doi.org/10.1103/PhysRevB.56.14399>
- ⁷⁴ Kaiwen Chen, Xiangqi Liu², Jiachen Jiao, Muyuan Zou, Chengyu Jiang, Xin Li, Yixuan Luo, Qiong Wu, Ningyuan Zhang, Yanfeng Guo, and Lei Shu, *Evidence of Spin Density Waves in La₃Ni₂O_{7- δ}* , Phys. Rev. Lett. **132**, 256503 (2024). <https://doi.org/10.1103/PhysRevLett.132.256503>
- ⁷⁵ K. W. Chen, X. Q. Liu, Y. Wang, Z. Y. Zhu, J. C. Jiao, C. Y. Jiang, Y. F. Guo, L. Shu, *Evolution of magnetism in Ruddlesden-Popper bilayer nickelate revealed by muon spin relaxation*, arXiv:2412.09003. <https://doi.org/10.48550/arXiv.2412.09003>
- ⁷⁶ Dan Zhao, Yanbing Zhou, Mengwu Huo, Yu Wang, Linpeng Nie, Ye Yang, Jianjun Ying, Meng Wang, Tao Wu, and Xianhui Chen, *Pressure-enhanced spin-density-wave transition in double-layer nickelate La₃Ni₂O_{7- δ}* , Science Bulletin **70**, 1239 (2025). <https://doi.org/10.1016/j.scib.2025.02.019>
- ⁷⁷ Masataka Kakoi, Takashi Oi, Yujiro Ohshita, Mitsuharu Yashima, Kazuhiko Kuroki, Takeru Kato, Hidefumi Takahashi, Shintaro Ishiwata, Yoshinobu Adachi, Naoyuki Hatada, Tetsuya Uda, and Hidekazu Mukuda, *Multi-band Metallic Ground State in Multilayered Nickelates La₃Ni₂O₇ and La₄Ni₃O₁₀ Probed by ¹³⁹La-NMR at Ambient Pressure*, J. Phys. Soc. Jpn. **93**, 053702 (2024). <https://doi.org/10.7566/JPSJ.93.053702>
- ⁷⁸ Xiaoyang Chen, Jaewon Choi, Zhicheng Jiang, Jiong Mei, Kun Jiang, Jie Li, Stefano Agrestini, Mirian Garcia-Fernandez, Xing Huang, Hualei Sun, Dawei Shen, Meng Wang, Jiangping Hu, Yi Lu, Ke-Jin Zhou, and Donglai Feng, *Electronic and magnetic excitations in La₃Ni₂O₇*, Nat. Commun. **15**, 9597 (2024). <https://doi.org/10.1038/s41467-024-53863-5>
- ⁷⁹ Xiaolin Ren, Ronny Sutarto, Xianxin Wu, Jianfeng Zhang, Hai Huang, Tao Xiang, Jiangping Hu, Riccardo Comin, X. J. Zhou, and Zhihai Zhu, *Resolving the Electronic Ground State of La₃Ni₂O_{7- δ} Films*, Commun. Phys. **8**, 52 (2025). <https://doi.org/10.1038/s42005-025-01971-z>
- ⁸⁰ N. K Gupta, R. Gong, Y. Wu, M. Kang, C. T. Parzyck, B. Z. Gregory, N. Costa, R. Sutarto, S. Sarker, A. Singer, D. G. Schlom, K. M. Shen, and D. G. Hawthorn, *Anisotropic Spin Stripe Domains in Bilayer La₃Ni₂O₇*, Nat. Commun. **16**, 6560 (2025). <https://doi.org/10.1038/s41467-025-61653-w>
- ⁸¹ J. Luo, J. Feng, G. Wang, N. N. Wang, J. Dou, A. F. Fang, J. Yang, J. G. Cheng, Guo-qing Zheng, and R. Zhou, *Microscopic evidence of charge- and spin-density waves in La₃Ni₂O₇ revealed by ¹³⁹La-NQR*, Chinese Phys. Lett. **42**, 067402 (2025). <https://doi.org/10.1088/0256-307X/42/6/067402>
- ⁸² Haozhe Wang, Long Chen, Aya Rutherford, Haidong Zhou, and Weiwei Xie, *Long-Range Structural Order in a Hidden Phase of Ruddlesden-Popper Bilayer Nickelate La₃Ni₂O₇*, Inorg. Chem. **63**, 5020 (2024). <https://doi.org/10.1021/acs.inorgchem.3c04474>
- ⁸³ Guoqing Wu, J. J. Neumeier, and M. F. Hundley, *Magnetic susceptibility, heat capacity, and pressure dependence of the electrical resistivity of La₃Ni₂O₇ and La₄Ni₃O₁₀*, Phys. Rev. B **63**, 245120 (2001). <https://doi.org/10.1103/PhysRevB.63.245120>
- ⁸⁴ Zengjia Liu, Hualei Sun, Mengwu Huo, Xiaoyan Ma, Yi Ji, Enkui Yi, Lisi Li, Hui Liu, Jia Yu, Ziyong Zhang, Zhiqiang Chen, Feixiang Liang, Hongliang Dong, Hanjie Guo, Dingyong Zhong, Bing Shen, Shiliang Li, and Meng Wang *Evidence for charge and spin density waves in single crystals of La₃Ni₂O₇ and La₃Ni₂O₆*, Sci. China Phys. Mech. Astron. **66**, 217411 (2023). <https://doi.org/10.1007/s11433-022-1962-4>
- ⁸⁵ D.-K. Seo, W. Liang, M.-H. Whangbo, Z. Zhang, and M. Greenblatt, *Electronic Band Structure and Madelung Potential Study of the Nickelates La₂NiO₄, La₃Ni₂O₇, and La₄Ni₃O₁₀*, Inorg. Chem. **35**, 6396 (1996). <https://doi.org/10.1021/ic960379j>
- ⁸⁶ Yanghao Meng, Yi Yang, Hualei Sun, Sasa Zhang, Jianlin Luo, Liucheng Chen, Xiaoli Ma, Meng Wang, Fang Hong, Xinbo Wang, and Xiaohui Yu, *Density-wave-like gap evolution in La₃Ni₂O₇ under high pressure revealed by ultrafast optical spectroscopy*, Nat. Commun. **15**, 10408 (2024). <https://doi.org/10.1038/s41467-024-54518-1>
- ⁸⁷ Mingtao Li, Mingxin Zhang, Yiming Wang, Jiayi Guan, Nana Li, Cuiying Pei, N-Diaye Adama, Qingyu Kong, Yanpeng Qi, Wenge Yang, *Orbital Signatures of Density Wave Transition in La₃Ni₂O_{7- δ} and La₂PrNi₂O_{7- δ} RP-Nickelates Probed via in-situ X-ray Absorption Near-edge Spectroscopy*, arXiv:2502.10962. <https://doi.org/10.48550/arXiv.2502.10962>
- ⁸⁸ Junjie Zhang, D. Phelan, A.S. Botana, Yu-Sheng Chen, Hong Zheng, M. Krogstad, Suyin Grass Wang, Yiming Qi, J.A. Rodriguez-Rivera, R. Osborn, S. Rosenkranz, M.R. Norman, and J.F. Mitchell, *Intertwined density waves in a metallic nickelate*, Nat Commun. **11**, 6003 (2020). <https://doi.org/10.1038/s41467-020-19836-0>
- ⁸⁹ Rustem Khasanov, Thomas J. Hicken, Igor Plokhikh, Vahid Sazgari, Lukas Keller, Vladimir Pomjakushin, Marek Bartkowiak, Szymon Królak, Michał J. Winiarski, Jonas A. Krieger, Hubertus Luetkens, Tomasz Klimczuk, Dariusz J. Gawryluk, and Zurab Guguchia, *Identical Suppression of Spin and Charge Density Wave Transitions in La₄Ni₃O₁₀ by Pressure*, arXiv:2503.04400.

- <https://doi.org/10.48550/arXiv.2503.04400>
- ⁹⁰ A. R. Moodenbaugh, Y. Xu, M. Suenaga, T. J. Folkerts, and R. N. Shelton, *Superconducting properties of $La_{2-x}Ba_xCuO_4$* , Phys. Rev. B **38**, 4596 (1988).
<https://doi.org/10.1103/PhysRevB.38.4596>
- ⁹¹ J. Sears, Y. Shen, M. J. Krogstad, H. Miao, E. S. Bozin, I. K. Robinson, G. D. Gu, R. Osborn, S. Rosenkranz, J. M. Tranquada, and M. P. M. Dean, *Structure of charge density waves in $La_{1.875}Ba_{0.125}CuO_4$* , Phys. Rev. B **107**, 115125 (2023).
<https://doi.org/10.1103/PhysRevB.107.115125>
- ⁹² X. Hu, P. M. Lozano, F. Ye, Q. Li, J. Sears, I. A. Zaloznyak, G. D. Gu, and J. M. Tranquada, *Charge density waves and pinning by lattice anisotropy in 214 cuprates*, Phys. Rev. B **111**, 064504 (2025).
<https://doi.org/10.1103/PhysRevB.111.064504>
- ⁹³ P. Abbamonte, A. Rusydi, S. Smadici, G. D. Gu, G. A. Sawatzky, and D. L. Feng, *Spatially modulated 'mottness' in $La_{2-x}Ba_xCuO_4$* , Nat. Phys. **1**, 155 (2005).
<https://doi.org/10.1038/nphys178>
- ⁹⁴ J. M. Tranquada, B. J. Sternlieb, J. D. Axe, Y. Nakamura, and S. Uchida, *Evidence for stripe correlations of spins and holes in copper oxide superconductors*, Nature **375**, 561 (1995).
<https://doi.org/10.1038/375561a0>
- ⁹⁵ M. Fujita, H. Goka, K. Yamada, J. M. Tranquada, and L. P. Regnault, *Stripe order, depinning, and fluctuations in $La_{1.875}Ba_{0.125}CuO_4$ and $La_{1.875}Ba_{0.075}Sr_{0.050}CuO_4$* , Phys. Rev. B **70**, 104517 (2004).
<https://doi.org/10.1103/PhysRevB.70.104517>
- ⁹⁶ M. Hücker, M. v. Zimmermann, G. D. Gu, Z. J. Xu, J. S. Wen, G. Xu, H. J. Kang, A. Zheludev, and J. M. Tranquada, *Stripe order in superconducting $La_{2-x}Ba_xCuO_4$ ($0.095 \leq x \leq 0.155$)*, Phys. Rev. B **83**, 104506 (2011).
<https://doi.org/10.1103/PhysRevB.83.104506>
- ⁹⁷ P. Corboz, T. M. Rice, and M. Troyer, *Competing states in the t - j model: Uniform d -wave state versus stripe state*, Phys. Rev. Lett. **113**, 046402 (2014).
<https://doi.org/10.1103/PhysRevLett.113.046402>
- ⁹⁸ Andrea Damascelli, Zahid Hussain, and Zhi-Xun Shen, *Angle-resolved photoemission studies of the cuprate superconductors*, Rev. Mod. Phys. **75**, 473 (2003).
<https://doi.org/10.1103/RevModPhys.75.473>
- ⁹⁹ Louis Taillefer, *Scattering and Pairing in Cuprate Superconductors*, Annu. Rev. Condens. Matter Phys. **1**, 51 (2010).
<https://doi.org/10.1146/annurev-conmatphys-070909-104117>
- ¹⁰⁰ B. Keimer, S. A. Kivelson, M. R. Norman, S. Uchida, and J. Zaanen, *From quantum matter to high-temperature superconductivity in copper oxides* *From quantum matter to high-temperature superconductivity in copper oxides*, Nature **518**, 179 (2015).
<https://doi.org/10.1038/nature14165>
- ¹⁰¹ K. Y. Chen, N. N. Wang, Q. W. Yin, Y. H. Gu, K. Jiang, Z. J. Tu, C. S. Gong, Y. Uwatoko, J. P. Sun, H. C. Lei, J. P. Hu, and J.-G. Cheng, *Double Superconducting Dome and Triple Enhancement of in the Kagome Superconductor CsV_3Sb_5 under High Pressure*, Phys. Rev. Lett. **126**, 247001 (2021).
<https://doi.org/10.1103/PhysRevLett.126.247001>
- ¹⁰² F. H. Yu, D. H. Ma, W. Z. Zhuo, S. Q. Liu, X. K. Wen, B. Lei, J. J. Ying, and X. H. Chen, *Unusual competition of superconductivity and charge-density-wave state in a compressed topological kagome metal*, Nat. Commun. **12**, 3645 (2021).
<https://doi.org/10.1038/s41467-021-23928-w>
- ¹⁰³ Lixuan Zheng, Zhimian Wu, Ye Yang, Linpeng Nie, Min Shan, Kuanglv Sun, Dianwu Song, Fanghang Yu, Jian Li, Dan Zhao, Shunjiao Li, Baolei Kang, Yanbing Zhou, Kai Liu, Ziji Xiang, Jianjun Ying, Zhenyu Wang, Tao Wu, and Xianhui Chen, *Emergent charge order in pressurized kagome superconductor CsV_3Sb_5* , Nature **611**, 682 (2022).
<https://doi.org/10.1038/s41586-022-05351-3>
- ¹⁰⁴ Z. Guguchia, C. Mielke III, D. Das, R. Gupta, J.-X. Yin, H. Liu, Q. Yin, M. H. Christensen, Z. Tu, C. Gong, N. Shumiya, Md Shafayat Hossain, Ts. Gamsakhurdashvili, M. Elender, Pengcheng Dai, A. Amato, Y. Shi, H. C. Lei, R. M. Fernandes, M. Z. Hasan, H. Luetkens, and R. Khasanov, *Tunable unconventional kagome superconductivity in charge ordered RbV_3Sb_5 and KV_3Sb_5* , Nat. Commun. **14**, 153 (2023).
<https://doi.org/10.1038/s41467-022-35718-z>
- ¹⁰⁵ Haitao Yang, Zihao Huang, Yuhang Zhang, Zhen Zhao, Jinan Shi, Hailan Luo, Lin Zhao, Guojian Qian, Hengxin Tan, Bin Hu, Ke Zhu, Zouyouwei Lu, Hua Zhang, Jianping Sun, Jinguang Cheng, Chengmin Shen, Xiao Lin, Binghai Yan, Xingjiang Zhou, Ziqiang Wang, Stephen J. Pennycook, Hui Chen, Xiaoli Dong, Wu Zhou, and Hong-Jun Gao, *Titanium doped kagome superconductor $CsV_{3-x}Ti_xSb_5$ and two distinct phases*, Sci. Bull. **67**, 2176 (2022).
<https://doi.org/10.1016/j.scib.2022.10.015>
- ¹⁰⁶ Igor Plokhikh, Thomas J. Hicken, Lukas Keller, Vladimir Pomjakushin, Samuel H. Moody, Pascale Foury-Leylekian, Jonas J. Krieger, Hubertus Luetkens, Zurab Guguchia, Rustem Khasanov, and Dariusz Jakub Gawryluk, arXiv:2503.05287.
<https://doi.org/10.48550/arXiv.2503.05287>
- ¹⁰⁷ Peter Atkins, Julio de Paula, and James Keeler, *Physical Chemistry*, Published in Great Britain by Oxford University Press; ISBN: 9780198847816; <https://doi.org/10.1016/j.physc.2023.1354376>
- ¹⁰⁸ A. Amato, H. Luetkens, K. Sedlak, A. Stoykov, R. Scheuermann, M. Elender, A. Raselli, D. Graf, *The new versatile general purpose surface-muon instrument (GPS) based on silicon photomultipliers for μ SR measurements on a continuous-wave beam*, Rev. Sci. Instrum. **88**, 093301 (2017).
<https://doi.org/10.1063/1.4986045>
- ¹⁰⁹ A. Suter and B. Wojek, *Musrfit: A Free Platform-Independent Framework for μ SR Data Analysis*, Phys. Procedia **30**, 69 (2012).
<https://doi.org/10.1016/j.phpro.2012.04.042>
- ¹¹⁰ Juan Rodríguez-Carvajal, *Recent advances in magnetic structure determination by neutron powder diffraction* *Author links open overlay panel*, Physica B: **192**, 55 (1993).
[https://doi.org/10.1016/0921-4526\(93\)90108-I](https://doi.org/10.1016/0921-4526(93)90108-I)
- ¹¹¹ Alex Amato and Elvezio Morenzoni, *Introduction to Muon Spin Spectroscopy. Applications to Solid State and Material Sciences*, Springer Nature (2024). <https://doi.org/10.1007/978-3-031-44959-8>
- ¹¹² A. Schenck, *Muon Spin Rotation Spectroscopy: Principles and Applications in Solid State Physics*, Adam Hilger, Bristol, 1985.
- ¹¹³ A. Yaouanc and P. D. de Réotier, *Muon Spin Rotation, Relaxation, and Resonance*, Oxford Science Publications, 2011.

¹¹⁴ S. J. Blundell, R. De Renzi, T. Lancaster, F. L. Pratt (eds.) *Muon spectroscopy. An introduction*, Oxford: Ox-

ford University Press, 2022.